DMD Fast Forward. Published on September 6, 2007 as doi:10.1124/dmd.107.017236




# PROGRESS CURVE ANALYSIS OF CYP1A2 INHIBITION; A MORE INFORMATIVE APPROACH TO THE ASSESSMENT OF MECHANISM-BASED INACTIVATION?

D.A. FAIRMAN, C. COLLINS AND S. CHAPPLE

*Department of Pharmacokinetics, Dynamics and Metabolism, Pfizer Global Research and Development, Sandwich, Kent CT13 9NJ, UK (D.A.F., C.C) and School of Biological Sciences, University of Plymouth, Plymouth, PL4 8AA, UK (S.C).*

**Running Title**

Progress curve analysis of mechanism-based CYP1A2 inhibition.

**Corresponding Author**:

David Fairman, Department of Pharmacokinetics, Dynamics and Metabolism (IPC 664), Pfizer Global Research & Development, Ramsgate Road, Sandwich, Kent CT13 9NJ. UK

Telephone: +44 (0) 1304 644612

Fax: +44 (0) 1304 651987

E.Mail: David.Fairman@Pfizer.com

Text Pages: 13

Tables: 2

Figures: 6

References: 24

Abstract: 249

Introduction: 735

Discussion: 652

**Abbreviations**: CYP, cytochrome P450; DDI, drug-drug interaction; NCEs, novel chemical entities; $C_{max}$, maximal plasma concentration; AUC, plasma area under the curve; TI, therapeutic index; MBI, mechanism based inactivation, $K_{iapp}$, apparent initial reversible inhibition constant

DMD Fast Forward. Published on September 6, 2007 as DOI: 10.1124/dmd.107.017236
This article has not been copyedited and formatted. The final version may differ from this version.



**Abstract**

Mechanism-based CYP inactivation is defined as a time and NADPH dependent inactivation that is not reversible upon extensive dialysis. Current methodologies utilise dilution approaches to estimate the rate of inactivation and offer limited mechanistic insight and are significantly influenced by experimental conditions. We investigated the potential of progress curve analysis as this experimental design allows investigation of both the reversible ($K_{iapp}$) and irreversible ($K_I$, $k_{inact}$) components of the reaction mechanism. The human liver microsomal CYP1A2 inactivation kinetics of resveratrol, oltipraz, furafylline and dihydralazine (Fig. 2) were evaluated. The inactivation results for furafylline ($K_I$ 0.8 μM and $k_{inact}$ 0.16 $min^{-1}$) are within 2 fold to published data ($K_I$ 1.6 μM and $k_{inact}$ 0.19 $min^{-1}$). Resveratrol and dihydralazine results are within a 4.3 fold range of published data which compares well to ranges of estimates of these parameters across publications (e.g. furafylline has estimates ranging of $K_I$ from 1.6 to 22.3 μM and $k_{inact}$ from 0.19 to 0.87 $min^{-1)}$. This range of estimates highlights the potential caveats surrounding the existing methodologies that have been previously discussed in depth. In addition to these inactivation parameters, we have been able to demonstrate a variation in balance of reversible versus irreversible inhibition within these inactivators. Oltipraz and resveratrol have $K_{iapp}$ values similar to their $K_I$ indicating a significant early onset reversible inhibition whereas furafylline and dihydralazine are dominated by irreversible inactivation. This approach allows a more mechanistic investigation of an inactivator and in the future may improve the prediction of clinical drug-drug interactions (DDIs).

Clinical drug-drug interactions (DDIs) can pose significant challenges to the development of novel chemical entities (NCEs) into marketable agents. NCEs may become victims to interactions that increase their $C_{max}$ or AUC and reduce their therapeutic index (TI) or alternatively cause increases in exposure and erode the TI of co-administered drugs. The most common DDIs are likely due to reversible inhibition of hepatic cytochrome P450 enzymes (CYPs) (Lin and Lu, 2000). Alternatively a more complex process can occur where drugs are metabolised into intermediates that can irreversibly inactivate CYPs. This is known as mechanism based inactivation (MBI) and results in a dose and time dependent loss of CYP activity (Silverman, 1995). Subsequent recovery of CYP activity is entirely due to de novo synthesis of CYP protein. This process leads to a significant delay between withdrawal of the inactivator and recovery of metabolism. An example of a mechanism based clinical DDI involving CYP1A2 is the interaction between furafylline and caffeine, where co-administration increased the AUC of caffeine 7-10 fold accompanied by significant incidence of unacceptable side effects (Tarrus et al, 1987).

Significant success has been achieved in the prediction of clinical DDI from in vitro analysis of reversible CYP inhibitors (Brown et al., 2005; Ito et al., 2005; Obach et al., 2006). These methodologies allow accurate estimation of the likely magnitude of DDI utilising relatively simple in vitro techniques and scaling to humans using physiological parameters such as hepatic blood flow and plasma unbound fraction plus estimates of the fraction metabolised by the inhibited CYP.

Due to the clinical significance of MBI, there continues to be a drive for improving DDI predictions in this area. The reaction scheme for mechanism based inactivation is given in Fig. 1 (Walsh et al., 1978; Silverman, 1995). In brief, the

scheme describes a rapid, reversible pre-equilibrium complex (EI) which can then be activated to an intermediate form (EI') according to the rate constant $k_2$. This can then progress to either an irreversibly inactivated final complex (EI*), according to the rate constant $k_{4,}$ or metabolism of the inactivator to a metabolite (M) and the release of enzyme back into the active pool. The kinetic constants used to describe this process are the initial binding equilibrium $K_i$, the maximum inactivation rate constant $k_{inact}$ and the concentration of inactivator required to achieve the half maximal rate of inactivation $K_I$.

**FIG. 1.**

Conventional in vitro inactivation studies utilise a pre-incubation step followed by dilution with a probe substrate to estimate remaining CYP activity. These experiments have utilised widely different experimental conditions, including pre-incubation time, dilution factor and activity measurement time, that makes comparison across studies and clinical predictions difficult (Ghanbari et al., 2006; Yang et al., 2005). Recent publications have demonstrated that in vitro data can be used to predict the magnitude of these interactions using a standardised pre-incubation and dilution methodology (Obach et al., 2007). While these methodologies are significantly improving the predictive power of in vitro studies they are still complicated to perform as the design has to be tailored in terms of pre-incubation times and dilution factor. These can have significant effects as any inactivation occurring post dilution will lead to inaccurate estimations of the kinetic constants especially if the initial velocities are not utilised (Ghanbari et al., 2006; Yang et al., 2005).

In this report we outline an alternative in vitro approach for the investigation of pre-steady state kinetics of CYP1A2 inactivation. Progress curve analysis utilises

an ‘all in’ approach where the enzyme is exposed simultaneously to probe substrate and inactivator/inhibitor whilst enzyme activity is monitored throughout the inactivation. This type of analysis has long been an accepted tool for measuring pre-steady state kinetics for a variety of physiological enzymes (Orson and Tipton, 1979, Pope et al., 1998, Maurer et al., 2000, Dash et al., 2001). However, its use in the context of CYP inactivation is unprecedented. Our goals were to demonstrate that this alternative approach can yield comparable data to the conventional dilution approach, may be less prone to analytical caveats and provide a more detailed interpretation of inactivation kinetics.

We investigated the time course of CYP1A2 inactivation with four precedented time dependent inactivators (Fig. 2): furafylline, dihydralazine, oltipraz and resveratrol plus a time independent inhibitor (paroxetine) (Von Moltke et al., 1996). These data were analysed to determine: mechanistic information around the inactivation mechanism, the key kinetic parameters for comparison to previous studies and, where appropriate, predictions of clinical DDI.

**FIG. 2.**

## Methods

**Materials.** Furafylline, dihydralazine, oltipraz, resveratrol, paroxetine and fluconazole were synthesised by Pfizer Global Research & Development (Sandwich, UK). Pooled human liver microsomes were supplied by BD-Gentest, Inc. (Woburn, MA). All other reagents were of the highest purity available and purchased from Sigma-Aldrich (Gillingham, UK).

**Inactivator time course studies.** Individual incubation mixes (total 1.7 ml) consisted of; phosphate buffer (50 mM pH 7.4), $MgCl_2$ (5 mM), NADPH regeneration system (5 mM isocitric acid & isocitric acid dehydrogenase at 1 unit/ml), human liver microsomes (HLM) (0.1 mg/ml microsomal protein), and CYP1A2 specific probe substrate (5 µM tacrine) (Spaldin V, 1995). The $K_m$ of tacrine in this batch of microsomes was previously determined to be 2µM (data not shown). Reactions were carried out at 37°C and initiated by the addition of NADPH (1 mM). Initial studies with rich data sampling in the early phase (data not shown) demonstrated that the turnover of tacrine (as monitored by determination of OH-tacrine production) becomes linear approximately 5 minutes after the addition of NADPH. Therefore, all incubations were left for 8 minutes after the addition of NADPH prior to addition of inactivator or MeOH vehicle. Immediately following mixing a 100 µl sample (representing $t_0$) was removed and quenched in ice cold acetonitrile (+0.05 % formic acid) containing internal standard (250 ng/ml fluconazole). Additional samples were removed at 11 further time points post addition of inactivator, where tacrine metabolism is linear (50 minutes).

DMD Fast Forward. Published on September 6, 2007 as DOI: 10.1124/dmd.107.017236
This article has not been copyedited and formatted. The final version may differ from this version.



Time course experiments were carried out to obtain inactivation progress curves with multiple concentrations (6-8) of each inactivator (0.5-3.5 µM furafylline, 20-150 µM dihydralazine, 0.5-20 µM oltipraz, 4-80 µM resveratrol) on 3-4 occasions. These concentrations were chosen to ensure a wide range of inactivation across the 50 minute time course. To account for inactivator depletion in the incubation, a time-averaged concentration was determined by trapezoidal integration using eq 1 in WinNonlin (Version 4.0.1; Pharsight, Mountain view, CA) (Zhao et al., 2004).

$$\text{Time averaged [I]} = \frac{\int_{t=0\,\text{min}}^{t=50\,\text{min}} I = [I]t \cdot dt}{50\,\text{min}} \quad (1)$$

Progress curve analysis was then carried out to estimate the key constants defined in equations 2 to 4 (Silverman, 1995, Yang et al., 2005).

$$K_i = (k_{-1} + k_2)/k_1 \quad (2)$$

$$k_{inact} = (k_2 \cdot k_4)/(k_2+k_3+k_4) \quad (3)$$

$$K_I = ((k_{-1} + k_2)/k_1) \cdot ((k_3+k_4)/(k_2+k_3+k_4)) \quad (4)$$

For each experiment non-linear regression of progress data was performed with equation 5, using Grafit (version 5) for each inactivator concentration. This regression simultaneously estimates the apparent rate constant for the formation of the final steady state equilibrium ($k_{obs}$) plus the initial and steady state velocities of product formation ($v_0$ and $v_S$) for each curve analysed (Morrison and Walsh, 1988, Pope et al., 1998).

$$[\text{Product}] = \frac{v_S \cdot t + (v_0 - v_S) \cdot (1 - e^{-k_{obs}\, t})}{k_{obs}} \quad (5)$$

DMD Fast Forward. Published on September 6, 2007 as DOI: 10.1124/dmd.107.017236
This article has not been copyedited and formatted. The final version may differ from this version.



Utilising this approach a set of data can be generated for each of these parameters against inactivator concentration. This process was repeated for each experimental day to generate 3-4 sets of data for further analysis.

Plots of $k_{obs}$ against inactivator concentration should yield hyperbolic profiles if inactivation is preceded by a saturable binding step and were analysed by non-linear regression (equation 6) to estimate $K_I$ and $k_{inact}$. I equals time averaged inactivator concentration as defined in equation 1.

$$k_{obs} = \frac{k_{inact} \cdot [I]}{K_I \cdot (1+S/K_m) + [I]} \quad (6)$$

Where a linear relationship is observed it indicates that, within the operating limits of the assays, we were unable to establish conditions where a saturable inactivation was observed. In this case a linear fit of the double reciprocal plot was utilised to estimate $K_I$ and $k_{inact}$ (Kitz and Wilson, 1962). For comparison purposes similar analyses were also undertaken for the compounds where hyperbolic profiles were obtained.

This methodology also allows estimates of the initial binding equilibrium as reflected in the magnitude of reduction of $v_0$ by the inactivator against respective vehicle control. While the overall mode of inhibition with each of these inactivators is mixed the contribution made by the inactivation process at this early time is likely to be minimal. Therefore, this inhibition is likely to reflect the initial rapid and reversible binding of the inactivator to the enzyme. As such this data can be used to generate a value close the initial rapid binding affinity that we have termed a $K_i$ apparent ($K_{iapp}$). Inhibition of $v_0$ was plotted against initial inactivator concentration and $IC_{50}$ values determined via standard methodologies then adjusted for substrate affinity and concentration using the Cheng-Prussof equation where $K_i$ =

$IC_{50}/(1+[S]/K_m)$. Paroxetine is a non-time dependent inhibitor and so was analysed by determining average velocity across the time course by linear fitting of each concentration. $IC_{50}$ values were then determined and $K_i$ estimated using Cheng Prusoff.

**Analytical Methods.** Quenched samples were centrifuged at 2000 g (4 $^oC$) for 40 minutes to pellet out precipitated protein. The supernatant (20 µl) was analysed for OH-tacrine and inactivator concentrations by LC-MS on an API4000 (MDS Sciex, Foster City, CA). Separation was achieved using an 8 minute gradient reverse phase method with a 50x4.6 mm Luna phenyl hexyl column (Phenomenex, Torrance, CA). The gradient was run from 100% MeOH:$H_20$ (10:90) to 100 % MeOH:$H_20$ 90:10, with both containing 2 mM ammonium acetate and 0.027 % formic acid and provided by Romil (Cambridge, UK).

DMD Fast Forward. Published on September 6, 2007 as DOI: 10.1124/dmd.107.017236
This article has not been copyedited and formatted. The final version may differ from this version.



## Results

Linearity of probe substrate turnover was observed in vehicle incubations up to 50 minutes, indicating that no significant loss of CYP1A2 activity occurs over the time course. For all the inactivators tested significant time and concentration dependent inactivation of CYP1A2 was observed. Paroxetine showed concentration but not time dependent inhibition consistent with its reported mechanism of competitive inhibition. Example progress curves for each of the inactivators are given in Fig. 3 with best fit lines to equation 5. All inactivator best fit lines reproducibly yielded $v_S$ values of zero consistent with essentially irreversible inactivation.

**FIG. 3**

Inactivator depletion was monitored during the experiments and time-averaged concentrations calculated as described by equation 1 (Table 1). Furafylline depletion was negligible (<2 %) so initial concentration was used for all analyses.

**Table 1.**

$k_{obs}$ was then plotted against time-averaged concentrations for each inactivator (Fig. 4). The linear relationship for dihydralazine and furafylline showed that we were unable to demonstrate the presence of a saturable step prior to inactivation. (Silverman, 1995).

**FIG. 4**

Double reciprocal analysis (Kitz and Wilson, 1962) was therefore utilised to generate estimates of $K_I$ and $k_{inact}$ (Fig. 5, Table 2). Oltipraz and resveratrol show the predicted hyperbolic relationship and fits to equation 6 enabled estimation of $K_I$ and $k_{inact}$. To enable comparison of the analysis methods, double reciprocal analysis was also performed for these compounds.

DMD Fast Forward. Published on September 6, 2007 as DOI: 10.1124/dmd.107.017236
This article has not been copyedited and formatted. The final version may differ from this version.



**FIG. 5**

Inhibition of $v_0$ was plotted against initial inactivator concentration assuming that at this stage minimal inactivator was depleted. Oltipraz and resveratrol showed significant inhibition across the concentration range thus enabling estimation of $K_{iapp}$ (Table 2; Fig. 6). Furafylline and dihydralazine were such weak inhibitors (<40 % inhibition at any concentration tested) that no estimation $K_{iapp}$ was possible.

**FIG 6**

**Table 2.**

DMD Fast Forward. Published on September 6, 2007 as DOI: 10.1124/dmd.107.017236
This article has not been copyedited and formatted. The final version may differ from this version.



**Discussion**

In this investigation we have been able to demonstrate the first use of progress curve analysis to investigate MBI of CYP1A2 inactivators. The furafylline data is within 2 fold of recently published dilution data generated within Pfizer laboratories with the same microsomal batch and near identical assay conditions (Obach et al., 2007) (Table 2). In this publication considerable attention has been spent on optimising assay conditions for each inactivator, in terms of pre-incubation and minimising post dilution inactivation, and therefore represents a relevant comparator.

Resveratrol and dihydralazine results are reasonably comparable to published data for $K_I$ and $k_{inact}$ (within 4.3 fold) especially given the published ranges for inactivation parameters across the literature. For example, furafylline has been cited as having a range of $K_I$ from 1.6 to 22.3 and $k_{inact}$ from 0.19 to 0.87 (Obach et al., 2007, Kunze and Trager, 1993). This range of estimate highlights the potential variations due to different microsomal batches and the caveats surrounding the existing analysis methodologies that have been discussed in depth and were the drivers for embarking on this investigation (Yang et al., 2005, Ghanbari et al., 2006). The results for oltipraz are not directly comparable as the literature values have been generated in a recombinant system (Chang et al., 2001).

Additionally a clear differentiation between the balance of initial reversible and time dependent inactivation in the compounds observed. Oltipraz and resveratrol show inhibition of $v_0$ that enabled estimation of the reversible $K_{iapp}$. When these are compared to the $K_I$, estimated either via hyperbolic plots of $k_{obs}$ against I or double reciprocal plots, the values are similar or $K_{iapp}$ is lower. This indicates that the rate of conversion of EI to the activated intermediate EI' ($k_2$) is likely to be the rate determining step in the overall inactivation process and that $k_1$ and $k_{-1}$ are relatively

DMD Fast Forward. Published on September 6, 2007 as DOI: 10.1124/dmd.107.017236
This article has not been copyedited and formatted. The final version may differ from this version.



fast. Conversely, the results for furafylline and dihydralazine show little inhibition of the initial velocity at any concentration and so $K_I$ is significantly lower than $K_{iapp}$. This indicates that, compared to resveratrol and oltipraz, $k_{2,}$ $k_1$ and $k_{-1}$ are relatively slow (Silverman., 1995). These data demonstrate that this analysis methodology can deliver a greater level of mechanistic insight than dilution methodologies. Reported studies have claimed the inactivation kinetics of resveratrol to be comparable with furafylline (Thomas et al., 2001). Indeed in this study both inactivators exhibit moderate potency and inactivation rate, however, the two can be distinguished based upon a different balance of reversible ($K_{iapp}$) and irreversible inactivation ($K_I$ and $k_{inact}$).

In recent years it has been well established that in vitro-in vivo correlations in the field of MBI are limited. Although modelling recommendations have been made to improve clinical DDI predictions (Obach et al., 2007), the caveats associated with the dilution approach have not been fully surmounted (Yang et al., 2005, Ghanbari et al., 2006). Progress curve analysis is capable of assessing multiple mechanisms of inhibition, and is not limited to MBI, although the focus of this study. Importantly, more confidence can be placed in the parameter estimates generated when we consider that the data is analysed in a way that captures the inactivation process as it occurs as opposed to deriving the degree of inactivation by dilution.

In summary this investigation has demonstrated that progress curve analysis can be successfully applied to investigate MBI of CYP1A2. Additionally this analysis allows a more in depth investigation of the balance of reversible and irreversible inactivation. Utilising this method the same magnitude of the furafylline/caffeine interaction is predicted using precedented methods (Obach et al., 2007). Future studies will examine a wider range of inactivators and CYPs to compare this

DMD Fast Forward. Published on September 6, 2007 as DOI: 10.1124/dmd.107.017236
This article has not been copyedited and formatted. The final version may differ from this version.



methodology to the dilution approach. Particular focus will be paid to inactivators and CYPs where a significantly greater sensitivity to $K_I$ and $k_{inact}$ estimates is predicted than the furafylline caffeine interaction. In parallel more powerful analysis and modelling techniques may be able to further utilise the added mechanistic insight offered.

DMD Fast Forward. Published on September 6, 2007 as DOI: 10.1124/dmd.107.017236
This article has not been copyedited and formatted. The final version may differ from this version.



**Acknowledgements.**

Thanks to our colleagues; Barry Jones, Ruth Hyland, Kuresh Youdim, Neil Benson and Maurice Dickins for support and advice throughout this investigation.

**References**

Brown HS, Ito K, Galetin A and Houston JB (2005) Prediction of in vivo drug-drug interactions from in-vitro data: impact of incorporating parallel pathways of drug elimination and inhibitor absorption rate constant. *Br J Clin Pharmacol* **60**:508-518.

Chang TKH, Chen J and Lee WBK (2001) Differential inhibition & inactivation of Human CYP1 enzymes by trans resveratrol: Evidence for Mechanism-based inhibition of CYP1A2. *J Pharmacol Exp Ther* **299**:874-882.

Dash C, Phadtare S, Deshpande V and Rao M (2001) Structural and mechanistic insight into the inhibition of aspartic proteases by a slow-tight binding inhibitor from an extremophilic *Bacillus* sp.: Correlation of the kinetic parameters with the inhibitor induced conformational changes. *Biochemistry* **40**:11525-11532.

Ghanbari F, Rowland-Yeo K, Bloomer JC, Clarke SE, Lennard MS, Tucker GT, and Rostami-Hodjegan A (2006) A critical evaluation of the experimental design of studies of mechanism based enzyme inhibition, with implications for in vitro to in vivo extrapolation. *Curr Drug Metab* **7**:315-334.

Ito K, Halifax D, Obach RS and Houston JB (2005) Impact of parallel pathways of drug elimination and multiple cytrochrome P450 involvement on drug-drug interactions: CYP2D6 paradigm. *Drug Met Disp* **33**:837-844.

Kitz R and Wilson IB (1962) Esters of methanesulfonic acid as irreversible inhibitors of acetycholinesterase. *J Biol Chem* **237**:3245-3249.

Kunze KL and Trager WF (1993) Isoform-selective mechanism-based inhibition of human cytochrome P450 1A2 by furafylline. *Chem Res Toxicol*. **6**:646-656.

Langouet S, Furge .L, Kerriguy N, Nakamura K, Guillouzo, A and Guengerich FP (2000) Inhibition of human cytochrome P450 enzymes by 1,2-dithiole-3-thione, oltipraz & its derivatives, and sulphaphane. *Chem Res Toxicol.* **13**:245-252.

Lin JH and Lu AYH (1998) Inhibition and induction of cytochrome P450 and the clinical implications. *Clin Pharmacokinet.* **35**:361-390.

Masubuchi Y and Horie T (1999) Mechanism-based inactivation of cytochrome P450s 1A2 & 3A4 by dihydralazine in human liver microsomes. *Chem Res Toxicol.* **12**:1028-1032.

Maurer ST, Tabrizi-Fard and Fung HL (2000) Impact of mechanism-based inactivation on inhibitor potency: implications for rational drug discovery. *J Pharm Sci*. **89**:1404-1412.

Morrison JF and Walsh CT (1988) The behavior and significance of slow-binding enzyme inhibitors. *Adv Enzymol Related Areas Mol Biol* **61**:201-301.

Obach RS, Walsky RL, Venkatakrishnan K, Gaman EA, Houston BJ and Tremaine LM (2006) The utility of in vitro cytrochrome P450 inhibition data in the prediction of drug-drug interactions. *J Pharmacol Exp Ther* **316**:336-348.

Obach RS, Walsky RL, and Venkatakrishnan K (2007) Mechanism-based inactivation of human cytrochrome P450 enzymes and the prediction of drug-drug interactions. *Drug Met Disp* **35**:246-255.

Orson BA and Tipton KF (1979) Kinetic analysis of progress curves. *Method. Enzymol* **63**:159-183.

Pope AJ, Moore KJ, McVey M, Mensah L, Benson N, Osbourne N, Broom N, Brown MJB and O'Hanlon P (1998) Characterization of isoleucyl-tRNA synthetase from *Stapylococcus aureus*. *J Biol Chem* **273**:31691-31701.

Silverman RB (1995) Mechanism-based enzyme inactivators. *Methods Enzymol* **249**:240-283.

Spaldin V, Madden S, Adams DA, Edwards RJ, Davies DS and Park BK (1995) Determination of human hepatic cytochrome P4501A2 activity in vitro use of tacrine as an isoenzyme-specific probe. *Drug Met Disp* 23(9):929-934

Tarrus E, Cami J, Roberts DJ, Spickett RGW, Celdran E and Segura J (1987) Accumulation of caffeine in healthy volunteers treated with furafylline. *Br J Clin Pharmacol* **49**:49-58.

Thomas KH, Chang JC, and Lee WBK (2001) Differential inhibition and inactivation of human CYP1 enzymes by trans-resveratrol: Evidence for mechanism-based inactivation of CYP1A2. *J Pharmacol Exp Ther* 299:874-882.

Von Moltke LL, Greenblatt DJ, Duan SX, Schmider J (1996) Phenacetin O-deethylation by human liver microsomes in vitro:inhibition by chemical probes, SSRI antidepressants, nefazodone and venlafaxine. *Psychopharmacology* 128(4):398-407

Walsh C, Cromartie T, Marcotte P and Spencer R (1978) Suicide substrates for flavoprotein enzymes. *Methods Enzymol* **53**:437-448.

Yang J, Jamei M, Rowland-Yeo K, Tucker GT, and Rostami-Hodjegan A (2005) Kinetic values for mechanism–based enzyme inhibition: Assessing the bias introduced by the conventional experimental protocol. *Eur J. Pharm Sci* **26**:334-340.

Zhao P, Kunze KL, and Lee CA (2004) Evaluation of time-dependent inactivation of CYP3A in cryopreserved human hepatocytes. *Drug Met Disp* **33**(6):853-861.

DMD Fast Forward. Published on September 6, 2007 as DOI: 10.1124/dmd.107.017236
This article has not been copyedited and formatted. The final version may differ from this version.



**Figure 1.** Generalised scheme for the mechanism based inactivation of CYP1A2. E; CYP1A2, I: inactivator, EI: reversible complex, EI': activated complex, EI*: inactivated complex M: metabolite of inactivator.

**Figure 2.** Chemical structures of furafylline, dihydralazine, oltipraz, resveratrol and paroxetine.

**Figure 3.** Plots of progress curves for CYP1A2 inactivation by 20-150 μM dihydralazine (A), 0.5-3.5 μM furafylline (B), 0.5-20 μM oltipraz (C), 4-80 μM resveratrol (D) and 1-12 μM paroxetine (E). Lines in A-D indicate best fit to equation 4 and show increasing inactivation with time and concentration of inactivator. Paroxetine shows no time dependent inhibition and lines indicate linear best fits.

**Figure 4.** Plots of $k_{obs}$ against time-averaged inactivator concentration for dihydralazine(A), furafylline (B), oltipraz (C), and resveratrol (D). A and B show linear fits, C and D show best fit according to equation 5.

**Figure 5.** Double reciprocal plots and best fit lines of $k_{obs}$ against time-averaged inactivator concentration for dihydralazine (A), furafylline (B), oltipraz (C), and resveratrol (D).

**Figure 6.** Inhibition of $v_0$ against inactivator concentration for oltipraz (A), resveratrol (B) and paroxetine (C). Solid lines represent best fit to a 2-parameter inhibition curve fixed from 0-100% inhibition.

DMD Fast Forward. Published on September 6, 2007 as DOI: 10.1124/dmd.107.017236
This article has not been copyedited and formatted. The final version may differ from this version.



TABLE 1
Time-averaged concentration for CYP1A2 inactivators. Furafylline concentrations were unchanged throughout the incubation at all concentrations.

| | Initial inactivator concentration (μM) | Time averaged concentration (μM) |
|---|---|---|
| Resveratrol | 4 | 3.3 |
| | 6 | 4.7 |
| | 10 | 8.7 |
| | 15 | 11 |
| | 40 | 34 |
| | 60 | 40 |
| | 80 | 60 |
| Oltipraz | 0.5 | 0.3 |
| | 1 | 0.5 |
| | 2 | 1.2 |
| | 5 | 3.5 |
| | 7.5 | 5.6 |
| | 10 | 7.9 |
| | 20 | 18 |
| Dihydralazine | 5 | 2.1 |
| | 10 | 4.6 |
| | 15 | 5.4 |
| | 25 | 8.5 |
| | 75 | 49 |
| | 100 | 66 |
| | 150 | 114 |

TABLE 2
Summarised constants defining CYP1A2 inactivator kinetics. Mean (s.e.m) n=3-4. ND not determined. NA not applicable.

| Inactivator | [I] vs $v_o$ | $k_{obs}$ vs [Inhibitor] plots | | | Double reciprocal plots | | | Published data | | |
|---|---|---|---|---|---|---|---|---|---|---|
| | $K_{iapp}$ (μM) | $K_I$ (μM) | $k_{inact}$ ($min^{-1}$) | $k_{inact\ t}$/ $K_I$ ($min^{-1}$/ml/μmol) | $K_I$ (μM) | $k_{inact}$ ($min^{-1}$) | $k_{inact}$ / $K_I$ ($min^{-1}$/ml/μmol) | $K_I$ (μM) | $k_{inact}$ ($min^{-1}$) | Ref |
| Oltipraz | 0.24 (0.05) | 0.41 (0.06) | 0.037 (0.004) | 100 (24) | 0.18 (0.03) | 0.033 (0.004) | 196 (18) | 9* | 0.19* | Langouet *et al*., 2000 |
| Resveratrol | 3.3 (0.5) | 2.2 (0.4) | 0.08 (0.01) | 41 (4) | 3.3 (1.0) | 0.09 (0.02) | 31 (8) | 8.5 | 0.28 | Chang *et al*., 2001 |
| Furafylline | ** | ND | ND | ND | 0.8 (0.2) | 0.16 (0.02) | 229 (39) | 1.6 | 0.19 | Obach et al., 2007+ |
| Dihydralazine | >45 | ND | ND | ND | 11 (5) | 0.13 (0.02) | 18 (7) | 42 | 0.03 | Masabuchi *et al*., 1999 |
| Paroxetine++ | 1.4 | NA | NA | NA | NA | NA | NA | NA | NA | |

* recombinant CYP1A2.
** $K_i$ not determined as inhibition <40% at highest concentration tested.
+ Carried out within Pfizer laboratories with identical microsomal batch and similar incubation conditions.
++ Non-time dependent inhibitor.

# Figure 1.

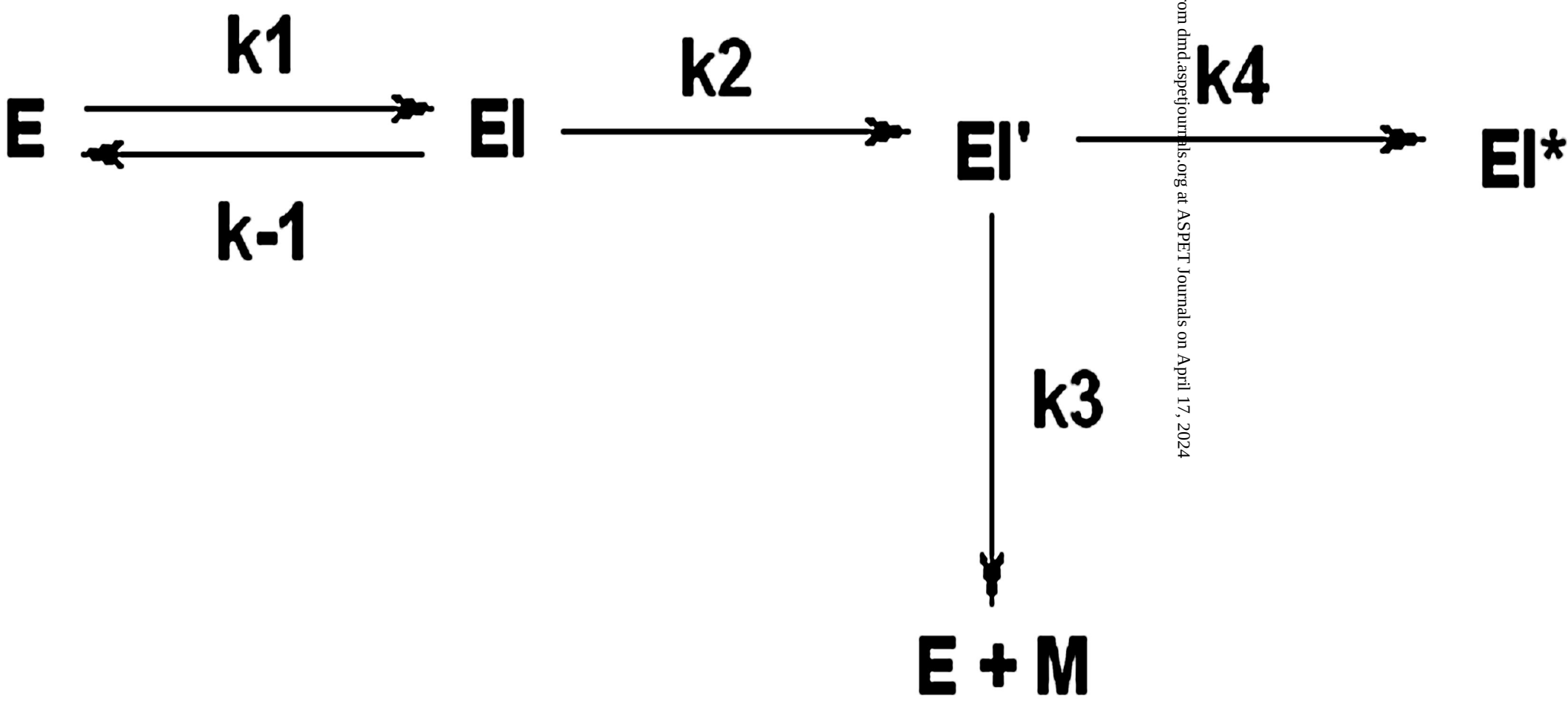

# Figure 2.

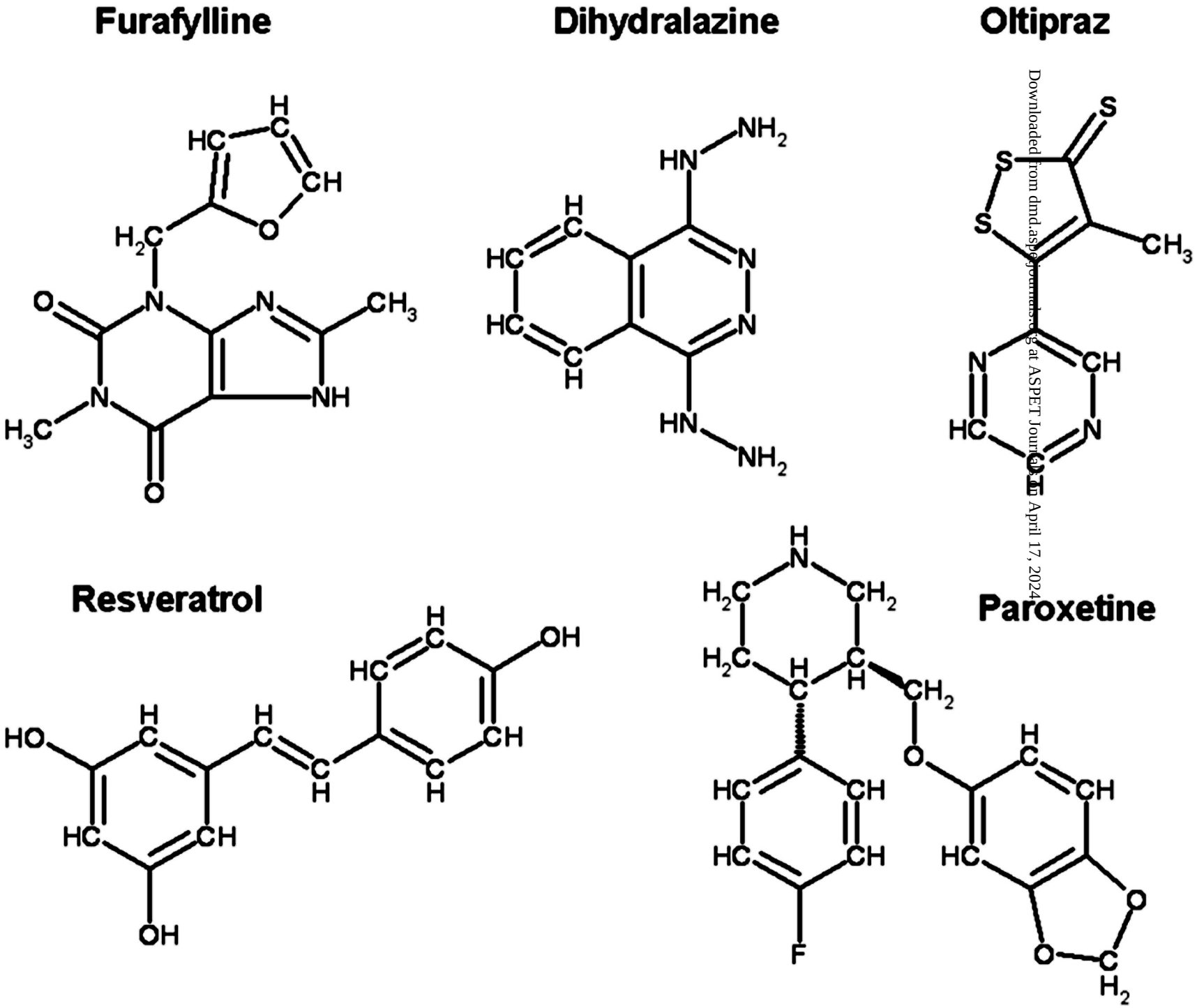

# Figure 3.

DMD Fast Forward. Published on September 6, 2007 as DOI: 10.1124/dmd.107.017236


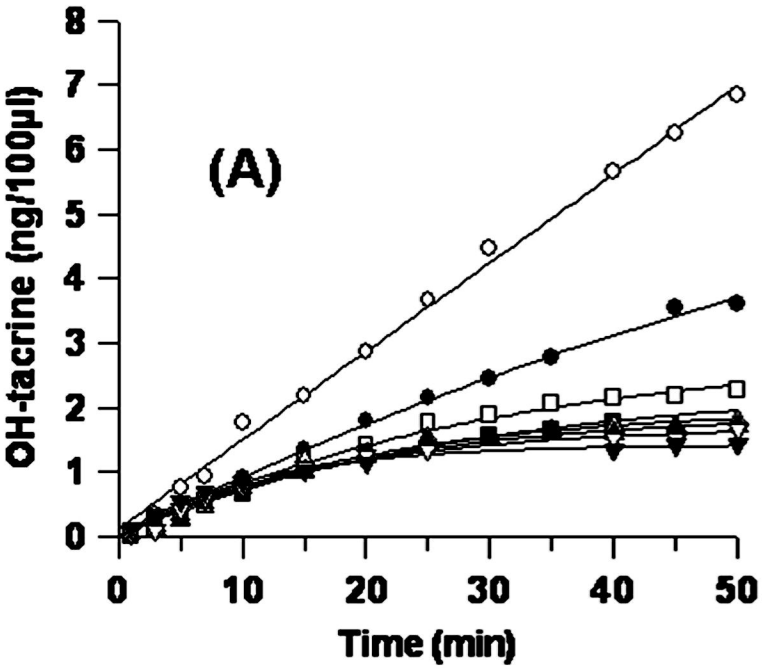


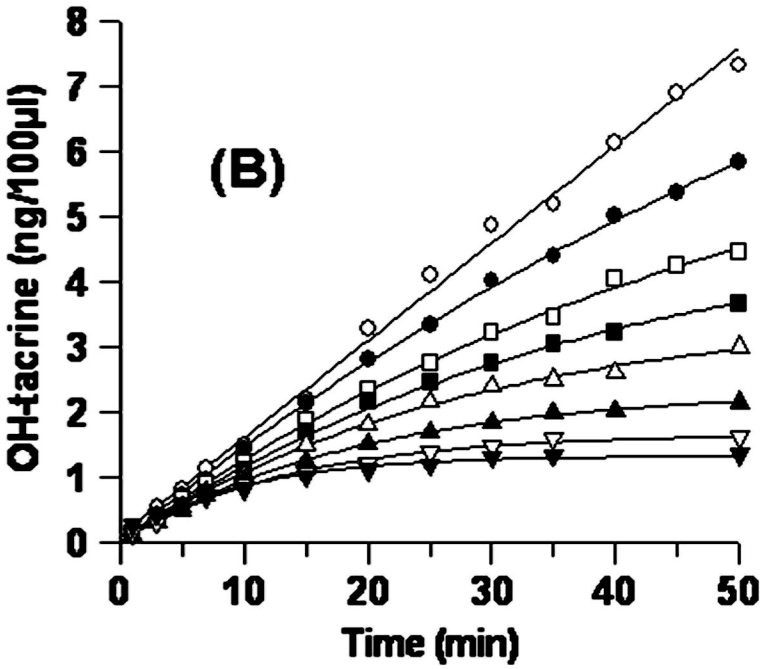


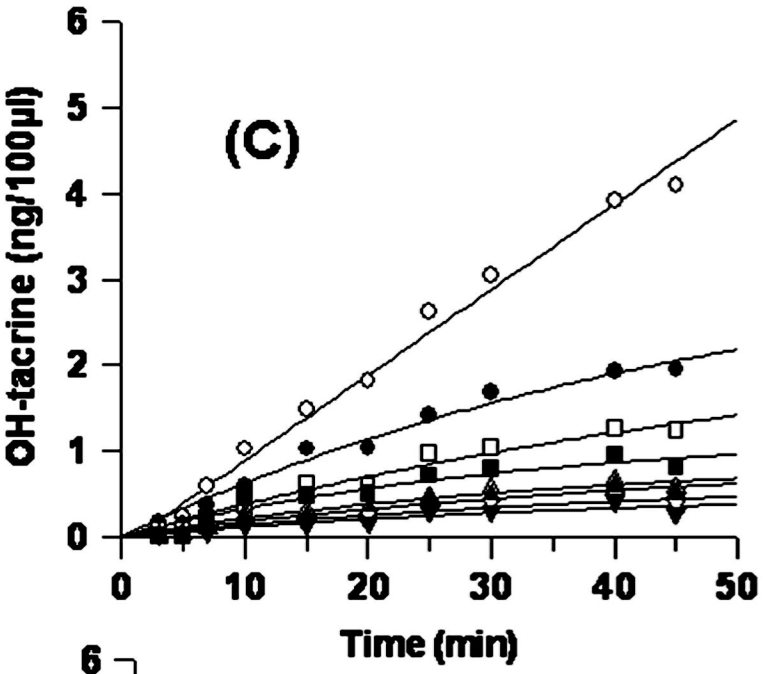


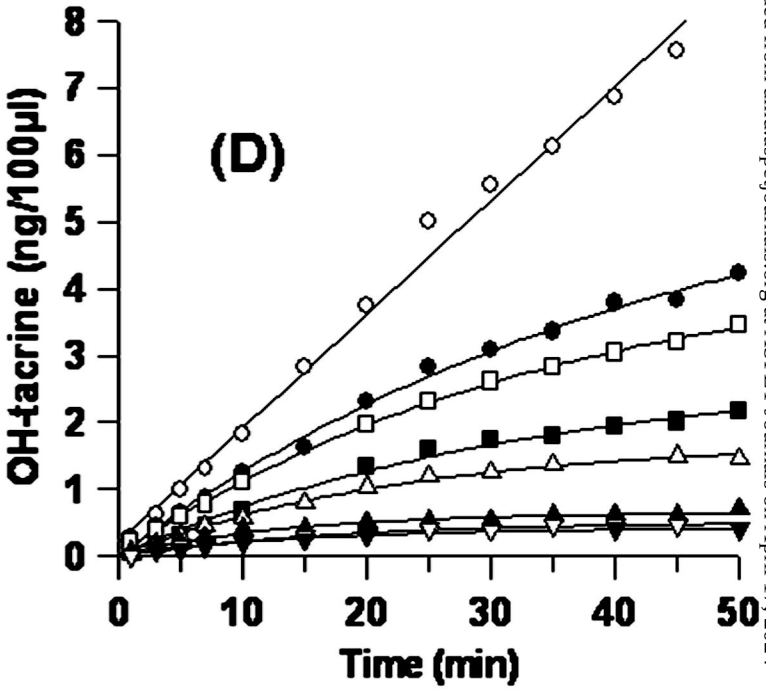


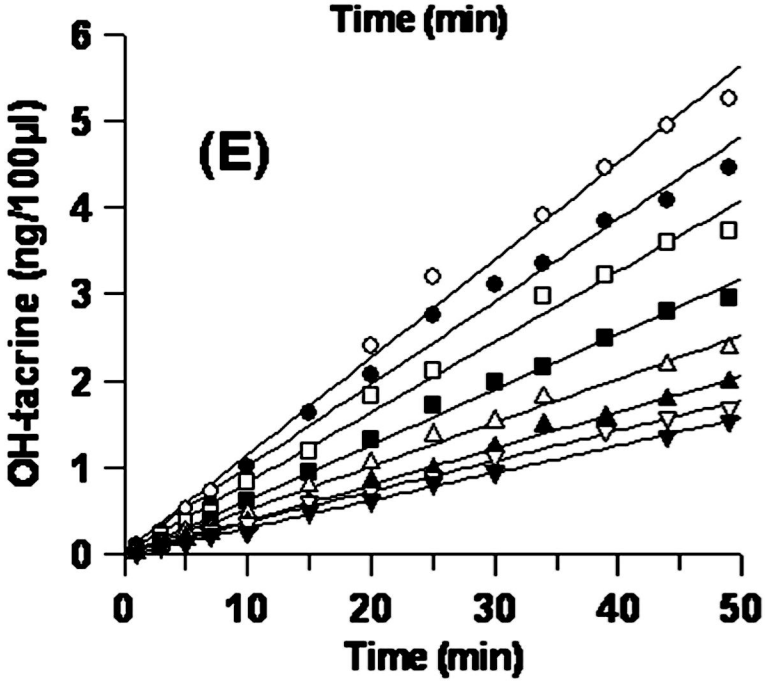

# Figure 4.

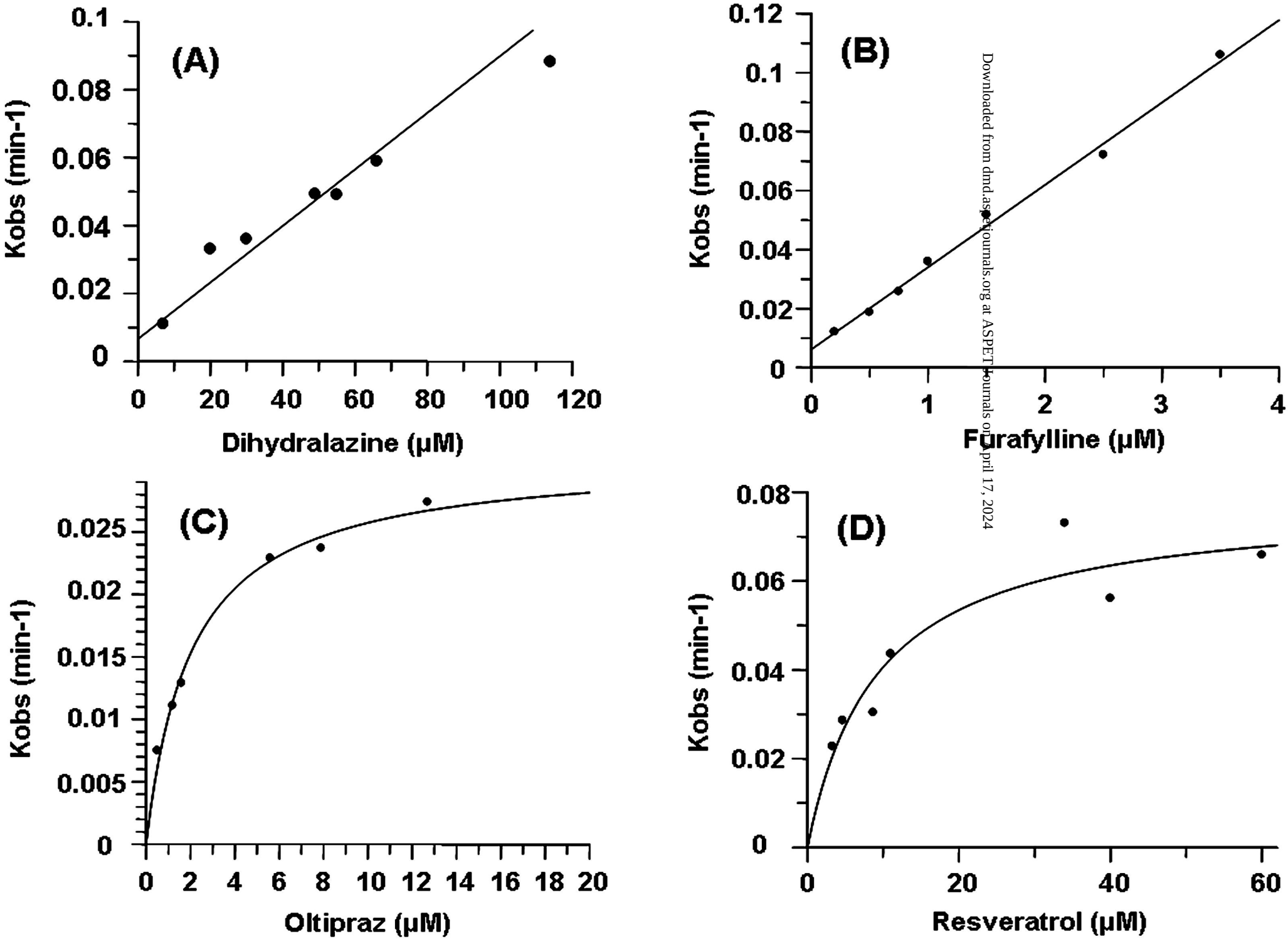

# Figure 5.

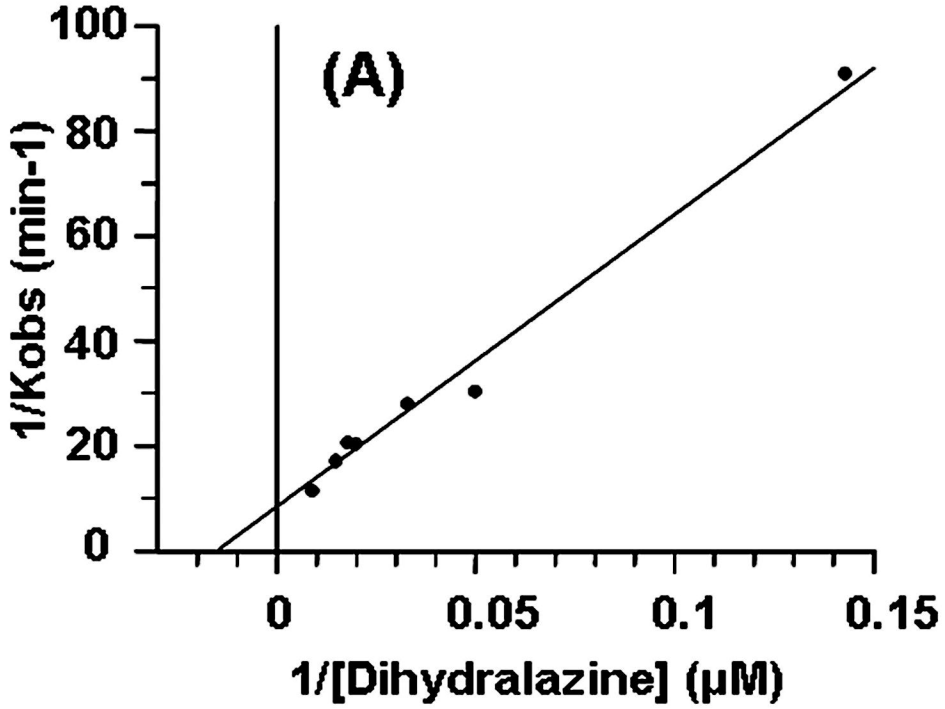


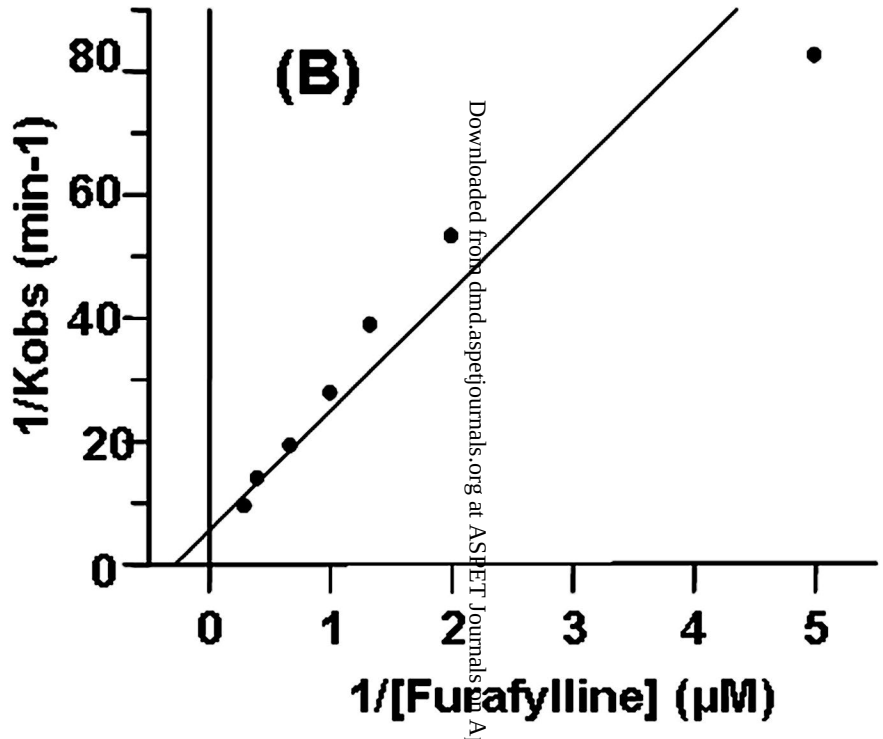


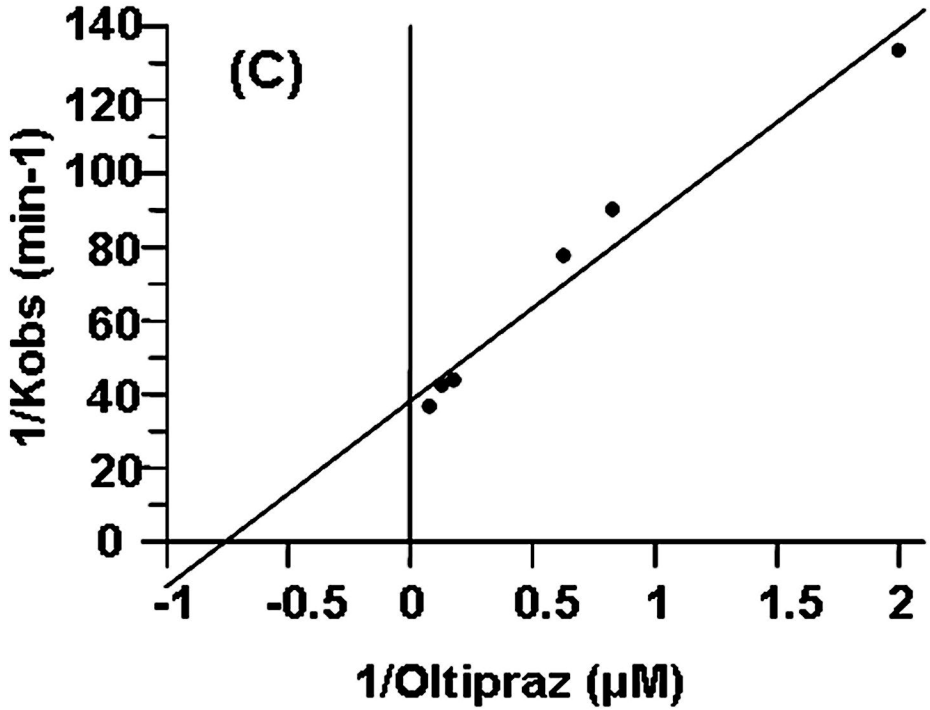


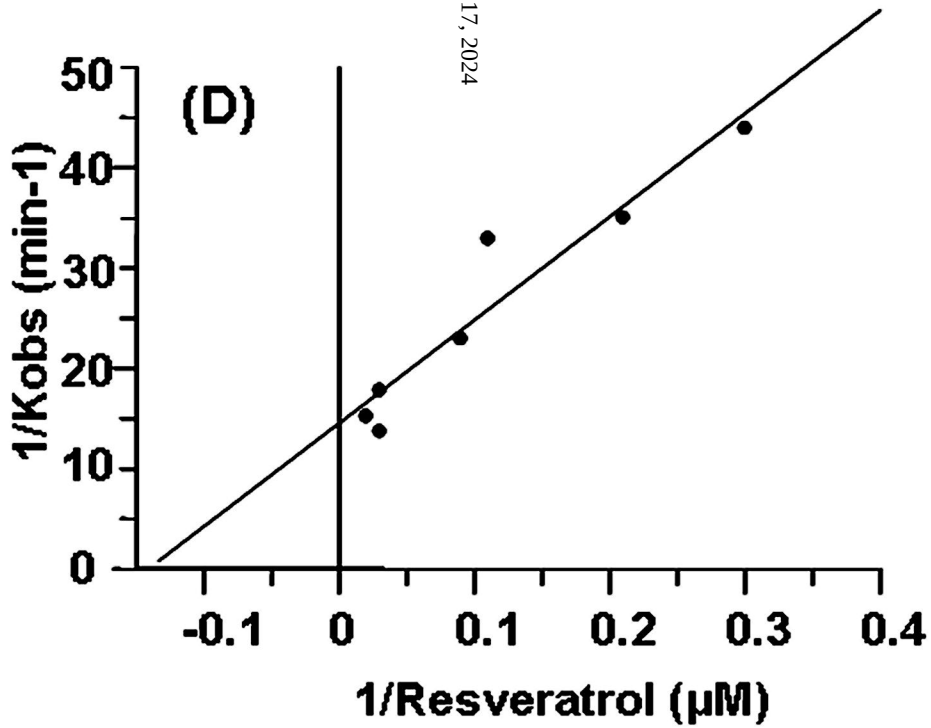

# Figure 6.